

Trigger, Reconstruction and Physics Performances in LHCb

C.Lazzeroni. For the LHCb Collaboration

Cavendish Laboratory, JJ Thomson Avenue, Cambridge, CB3 0HE, United Kingdom

Abstract. The LHCb experiment at LHC is a single-armed spectrometer designed to pursue extensive, high precision studies of CP violation and rare phenomena in b hadron decays. In this contribution, the trigger and reconstruction performance are summarised, and the expected performance for selected b physics measurements is discussed.

Keywords: LHCb, Trigger, Reconstruction, b Physics, CP Violation, Rare decays of b hadrons

PACS: 13.20.He, 14.65.Fy, 29.85.+c

INTRODUCTION

LHCb is one of the four major experiments that will take data at the LHC, due to start operation in 2007. The primary aims of LHCb are to perform precision tests of CP violation and to search for new physics in b hadron decays. About 10^{12} $b\bar{b}$ pairs will be produced in LHCb per 10^7 seconds (a nominal year) in pp collisions with a luminosity of $2 \times 10^{32} \text{ cm}^{-2}\text{s}^{-1}$. A large, high-purity sample of b hadrons, decaying in a variety of channels, will be accumulated. LHCb will perform a detailed study of B meson mixing, precise measurements of the angles of the unitary triangle and investigations of rare decays in b hadrons, looking for new physics in loop-induced processes.

The LHCb detector is optimised to reach these physics goals. Here a brief description of the reconstruction performance is given, and the sensitivities in typical channels for the study of B_s mixing, CP violation and rare decays are summarised.

TRIGGER AND EVENT RECONSTRUCTION PERFORMANCE

At the LHC energies, the production of b and \bar{b} quarks is predominantly along the beam axis, and highly correlated with each other, so that if one b goes forward into the detector acceptance, the corresponding \bar{b} products are also captured with high probability. This leads to high efficiency for a single arm spectrometer design, like LHCb, where only a factor ~ 2 is lost compared to a twin-arm spectrometer. Moreover, owing to an extended acceptance in the forward direction (higher η), a factor 2 better $b\bar{b}$ cross section is expected at LHCb compared to the ATLAS and CMS experiments. At the LHCb luminosity, events are dominated by single proton-proton interactions and the occupancy in the detector remains low.

The LHCb detector comprises a beam pipe, a Vertex Locator, a tracking system with a dipole magnet, two Ring Imaging Cherenkov detectors, an electromagnetic and a hadronic calorimeter and a muon system. To achieve its physics goals, efficient trigger, exclusive signal reconstruction, good proper time resolution and flavour tagging are essential for LHCb. For a detailed description of the detector, see [1, 2, 3, 4, 5, 6]. For an update on the installation and commissioning status, see [7].

Trigger

The experiment will use various levels of trigger to reduce the 10 MHz rate of visible interactions to the 2 kHz that will be stored. The b -quark production cross section of ~ 0.5 mb at $\sqrt{s} \sim 14$ TeV pp interactions is only a small fraction of the total visible cross section of ~ 100 mb. The LHCb trigger fully exploits the b -decay topology, characterised by significant transverse momentum due to the high b -quark mass, and long lifetime yielding large impact parameter (IP) values. The first level trigger (Level 0, hardware) relies on high- p_T e, γ, π^0, μ, h candidates, decreasing the rate to 1 MHz. The higher level trigger (HLT) is software based and makes use of the full detector information. Four independent trigger streams are defined, depending on the Level 0 output: $\mu, \mu + h, h$, and $ecal$ streams. The p_T and

IP discriminations are then used to reduce the output to 2 kHz. The overall trigger efficiency varies from 30% to 80% depending on the signal channels.

Reconstruction

Exclusive decay reconstruction requires good mass resolution, which is linked to excellent momentum resolution. For tracks with a momentum higher than 10 GeV/c the average efficiency is $\sim 95\%$, tuned to have a ghost rate of $\sim 4\%$ for $p_t > 0.5$ GeV/c [8]. The average track momentum resolution is $\delta p/p = 0.37\%$.

The proper time of a b hadron decay is determined from the distance between its production and decay vertex and from its momentum. Using a double Gaussian fit to the distribution of the vertex residuals, the resolution on the primary vertex position along the beam direction (z coordinate) is measured to be $44 \mu\text{m}$, with 22% of the events being in the second Gaussian which is $124 \mu\text{m}$ wide (see Fig. 1 (left)). A resolution of $168 \mu\text{m}$ is obtained for the $B_s \rightarrow D_s K$ decay vertex, taken as an example, using a simple Gaussian fit (see Fig. 1 (centre)). Therefore, the proper time resolution is usually dominated by the resolution on the B decay vertex. The proper time resolution for the same decay is shown in Fig. 1 (right). Using a double Gaussian fit the core resolution is measured to be $33 fs$. The second Gaussian accounts for 31% of the events and has a width of $67 fs$.

Efficient particle identification in the momentum range 2-100 GeV/c is needed for flavour tagging and background rejection. The average kaon identification efficiency for momenta between 2 and 100 GeV/c is 83% with a π mis-identification rate of 6%. Different optimisations can be performed, in order to improve the mis-identification rate at the expenses of the efficiency. A detailed review of tracking performance and particle identification can be found in [8].

Neutral particle reconstruction is performed using both resolved (separate) clusters and merged (overlapping) cluster shapes in the electromagnetic calorimeter. A mean efficiency of $\sim 53\%$ is obtained for $B^0 \rightarrow \pi^+ \pi^- \pi^0$ events, as shown in Fig. 2 (left) as a function of the π^0 transverse momentum. The π^0 mass resolution is shown in Fig. 2 (centre) and (right) for resolved and merged π^0 respectively.

As an example of the mass resolutions that can be achieved, the reconstructed D_s and B_s mass distributions for $B_s \rightarrow D_s(KK\pi)K$ events are shown in Fig 3 (left, centre). The mass resolutions are $\sim 5.5 \text{ MeV}/c^2$ for D_s and $\sim 14 \text{ MeV}/c^2$ for B_s . The second peak in the B_s distribution corresponds to $B_s \rightarrow D_s(KK\pi)\pi$ where the π has been mis-identified as a K .

The identification of the initial b-quark charge (flavour) of a reconstructed b hadron decay is performed using opposite-side and same-side tagging algorithms. To determine the flavour of the accompanying B, opposite-side tagging uses the charge of: a) leptons from a semileptonic decay; b) a kaon from a $b \rightarrow c \rightarrow s$ chain; c) the charge of all particles in a jet or at a vertex. Same-side tagging uses the charge of fragmentation particles which are correlated in phase space with the signal B meson to determine its flavour. Figure 7 (left) lists the tagging power ($\epsilon D^2 = \epsilon(1 - 2w)^2$), where ϵ is the tagging efficiency and w is the wrong tagging fraction) of each tagging category and the combined tagging power for B_d and B_s mesons. The range of values depends on the signal channel considered.

For further details on reconstruction performances, see [9].

PHYSICS PERFORMANCE

Selected baseline physics measurements are discussed below. All event samples were produced using the full detector simulation, realistic digitization and reconstruction with full pattern recognition and realistic trigger simulation. Toy Monte Carlo algorithms were used for sensitivity studies. The background was assumed to come from $b\bar{b}$ inclusive events, having similar topologies. All sensitivities are relative to one year of data taking or 10^7 s, equivalent to $2fb^{-1}$ accumulated statistics, unless otherwise specified. For the estimates of the background over signal ratio (B/S), the 90% CL is used throughout this paper.

$B_s \bar{B}_s$ mixing

The LHCb precision for measuring $B_s \bar{B}_s$ oscillations has been estimated using the decay $B_s \rightarrow D_s \pi$. A sample of 80k events ($B/S < 0.3$) will be collected per year of running, with a proper time resolution of $\sim 40 fs$. A clear observation

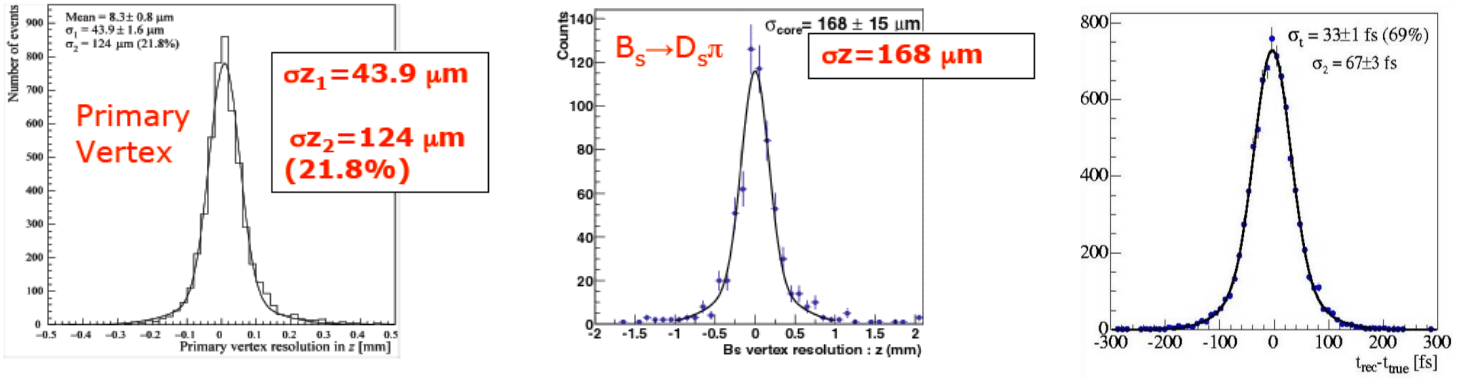


FIGURE 1. Primary vertex resolution (left), secondary vertex resolution (centre), proper time resolution (right).

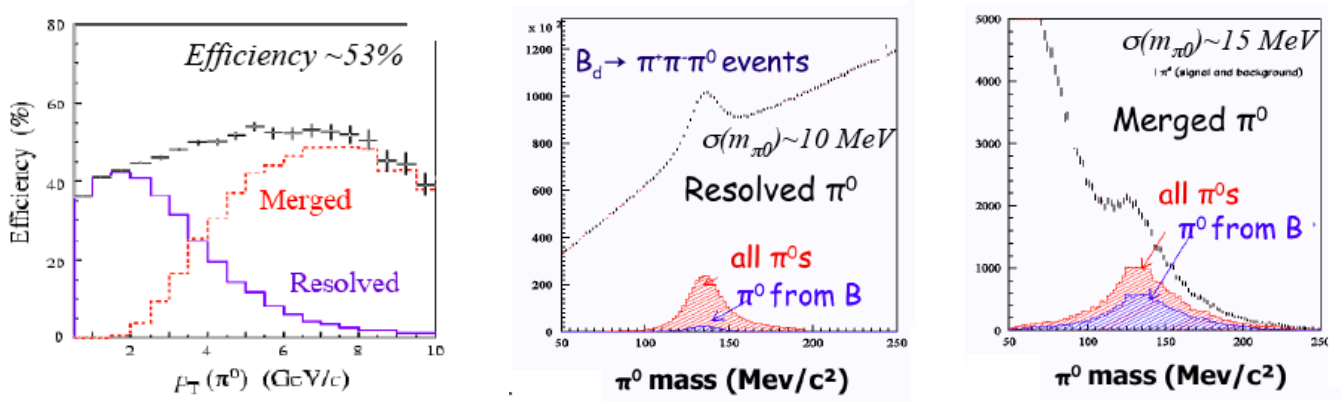


FIGURE 2. Efficiency for π^0 reconstruction as a function of p_T (left), π^0 mass resolution for resolved π^0 s (centre), π^0 mass resolution for merged π^0 s (right).

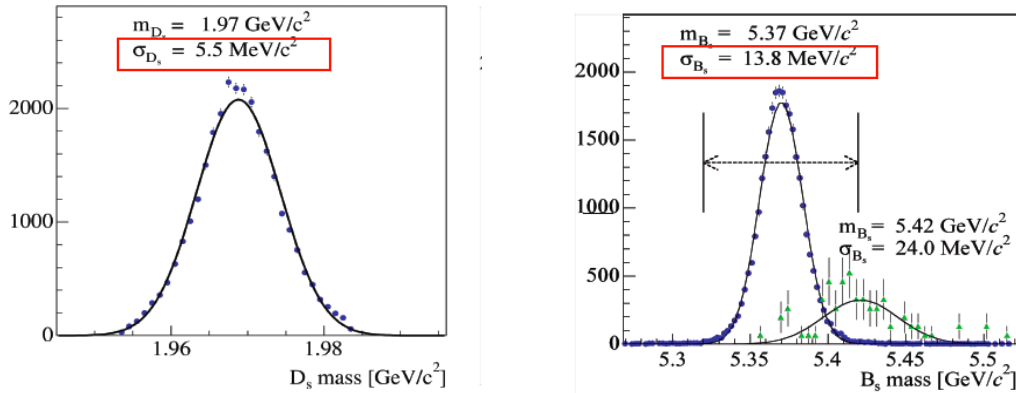


FIGURE 3. D_s mass resolution (left), B_s mass resolution (right). The arrow indicates the 3σ region.

of the oscillation pattern can be performed, as seen in Fig.4 (left). Given the value of Δm_s , recently measured [10, 11], LHCb will be able to measure it with much less than $2fb^{-1}$ of data, and a high precision measurement is expected in 1 year: $\sigma_{stat}(\Delta m_s) \sim 0.01 ps^{-1}$.

The $B_s \rightarrow J/\Psi\phi$ decay measures simultaneously $\phi_s = -2\chi$ and $\Delta\Gamma_s/\Gamma_s$, the oscillation phase and the decay width

difference between the two CP eigenstates. The values for those quantities predicted by the Standard Model are respectively -0.04 and 0.1. This decay mode provides high statistics ($\sim 120\text{k}$ events/year, $B/S < 0.33$), but requires partial wave analysis since it contains both CP-even and CP-odd contributions. The sensitivities after 1 year of running are $\sigma(\phi_s) \sim 0.03$ and $\sigma(\Delta\Gamma_s/\Gamma_s) \sim 0.02$; the first is comparable to the Standard Model prediction, while the second is significantly better. Using the CP modes $B \rightarrow J/\Psi\eta, \eta_c\phi$, the sensitivity is improved to $\sigma(\phi_s) \sim 0.013$ after 5 years.

Measurement of α and γ

LHCb will provide precise measurements of all the angles of the unitary triangle. Together with the excellent knowledge already obtained on the angle β from experiments at e^+e^- colliders, and the information available on the sides of the triangle, a measurement of the other two angles will over-constrain the unitary triangle and may allow detection of NP contributions to CP violation.

The sensitivity for the angle α has been studied using the decay $B_d \rightarrow \rho\pi$. A sample of 14k events will be reconstructed per year, with a selection based on multivariate analysis, and a ratio $B/S < 1$. Using a time-dependent Dalitz fit method [12], the angle α can be determined with one year of data to a precision of 10° (see Fig.4 (right) for the Dalitz plot).

The angle γ can be measured at LHCb using several methods.

The decay $B_s \rightarrow D_s K$, where only tree diagrams contribute, should provide a measurement of $\gamma - 2\chi$ free from new physics effects. The mixing phase 2χ will then be measured separately, as illustrated above. Here the K/π separation significantly suppresses reflections from $B_s \rightarrow D_s\pi$. An annual yield of 5.4k events is expected, with a ratio $B/S < 1$. The measurement of $\gamma - 2\chi$ will be performed using the time-dependent rates of $B_s \rightarrow D_s^+ K^-$ and $B_s \rightarrow D_s^- K^+$, and their charge conjugates (see Fig 5). For $\Delta m_s = 20\text{ps}^{-1}$ this measurement gives a precision $\sigma(\gamma)$ of 14° with 2fb^{-1} .

γ can be extracted from the interference of $B^\pm \rightarrow D^0 K^\pm$ and $B^\pm \rightarrow \bar{D}^0 K^\pm$ when D^0 and \bar{D}^0 decay to a common final state. The decay amplitude can be parameterised as $A(B^- \rightarrow \bar{D}^0 K^-) = A_B r_B e^{i(\delta-\gamma)}$ where $A_B = A(B^- \rightarrow D^0 K^-)$, r_B is the relative colour and CKM suppression between the two modes, and δ is the strong phase difference. Two types of decays are currently under study in LHCb: Cabibbo favoured self-conjugate decays (like $K_s\pi\pi$), the sensitivity of which is under study, and Cabibbo favoured/doubly Cabibbo suppressed modes (like $K\pi, K\pi\pi\pi$). The latter study is based on the ADS method [13, 14]: the relative rates of $B^+ \rightarrow DK^+$ and $B^- \rightarrow DK^-$ depend on the parameters γ , r_B , δ_B , r_D , δ_D . Taking $r_B = 0.15$, $\sim 60\text{k}$ $B^\pm \rightarrow D^0 K^\pm$ and $\sim 2\text{k}$ $B^\pm \rightarrow \bar{D}^0 K^\pm$ decays are expected in one year, and the sensitivity to γ is $\sigma(\gamma) \sim 5^\circ$ considering the background ($\sim 3.9^\circ$ with no background, see Fig. 5 (right) for an example of the fit results). The sensitivity with lower values of r_B is under study.

The decay $B_d \rightarrow D^0 K^{*0}$ also proceeds via a tree diagram, and has no sensitivity to new physics. The method [15] to extract γ is based on the measurement of six time-integrated decay rates for $B_d \rightarrow D^0 K^{*0}$, $B_d \rightarrow \bar{D}^0 K^{*0}$, $B_d \rightarrow D_{CP}^0 K^{*0}$ and their CP conjugates. Samples of about 3.4k $B_d \rightarrow \bar{D}^0(K^-\pi^+)K^{*0}$, 0.5k $B_d \rightarrow D^0(K^+\pi^-)K^{*0}$, and 0.6k $B_d \rightarrow D_{CP}^0(K^+K^-)K^{*0}$ decays will be reconstructed per year (see Table 7 (right)). The precision reached is $\sigma(\gamma) \sim 8^\circ$ with 2fb^{-1} .

γ can be measured from time-dependent asymmetries for $B_d \rightarrow \pi\pi$ and $B_s \rightarrow KK$ decays [16, 17, 18], where both penguin and tree diagrams contribute. This measurement is sensitive to new physics appearing in the penguin loops. Here again the K/π separation is crucial because of numerous reflections from $B_{d,s}$ and Λ_b decays. The asymmetries can be parameterised as $A_{CP} = A^{dir} \cos(\Delta mt) + A^{mix} \sin(\Delta mt)$. The four observables are functions of the parameters: γ , mixing phases ϕ_d and ϕ_s , ratios of penguin over tree contributions $P/T = de^{i\theta}$. Measuring ϕ_d and ϕ_s independently and assuming U-spin symmetry ($d_{\pi\pi} = d_{KK}$, $\theta_{\pi\pi} = \theta_{KK}$), the relations above reduce to four measured quantities with three unknowns, which can be solved for γ . The annual yield of 26k $B_d \rightarrow \pi\pi$ ($B/S < 0.7$) and 37k $B_s \rightarrow KK$ ($B/S < 0.3$) events allows a precision of $\sigma(\gamma) \sim 5^\circ$. Since the system is overconstrained, the hypothesis of U-spin conservation can be also tested.

Rare decays: $B \rightarrow K^* \mu\mu$

Rare loop-induced decays are sensitive to new physics in many Standard Model extensions. At LHCb, rare decays such as decay $B_d \rightarrow K^* \mu\mu$ will be studied. The expected annual yield is $\sim 4.5\text{k}$, with a ratio $B/S < 0.2$, using the Standard Model prediction for the branching ratio of $\sim 10^{-6}$. Further improvements are expected in the signal selection to enhance the yield.

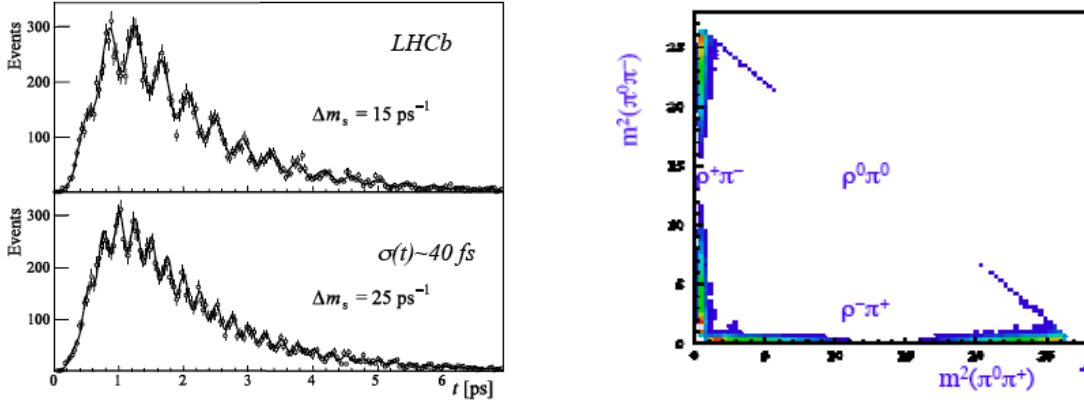


FIGURE 4. Distribution of $B_s \rightarrow D_s\pi$ proper time (ps) after 1 year of data taking, for $\Delta m_s = 15, 25 \text{ ps}^{-1}$ (left). Dalitz plot for the decay $B \rightarrow \pi^0\pi^+\pi^-$ (right).

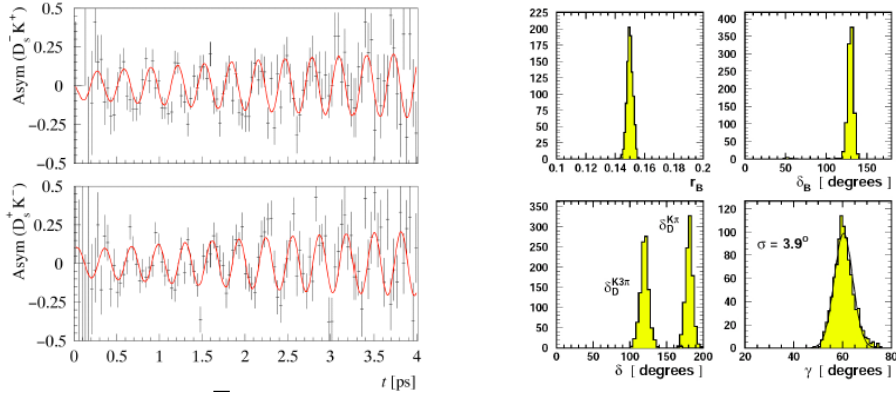


FIGURE 5. Distribution of $B_s \rightarrow D_s K$ asymmetry versus proper time (ps) for $D_s^+ K^-$ and $D_s^- K^+$ (left). Example of fit results for r_B , δ_B , δ_D and γ in $B^\pm \rightarrow D^0 K^\pm$ using the ADS method with no background.

This channel is well suited to searches for new physics, since New Physics models make definite predictions for the shape of the forward-backward asymmetry of the μ^+ in the $\mu\mu$ rest frame with respect to the B direction, as a function of the $\mu\mu$ invariant mass [19] (see Fig. 6 (left)). In particular the zero crossing of the forward-backward asymmetry is predicted with small theoretical uncertainties. With a year of data taking, a clear observation of NP should be possible; with 10 fb^{-1} the position of the zero should be located with a precision of $\pm 0.53 \text{ GeV}^2$ (see Fig 6 (right)).

CONCLUSIONS

Using a detailed simulation of the LHCb detector, we demonstrate that the LHCb experiment can efficiently reconstruct many different decay modes with a very good performance in the trigger, proper time resolution, mass resolution, and flavour tagging. This will allow LHCb to fully explore the B_s mixing, to extract CKM parameters with various methods, and to perform studies of rare decays. The experiment will make precision tests of the Standard Model in order to constrain, and possibly discover, new physics.

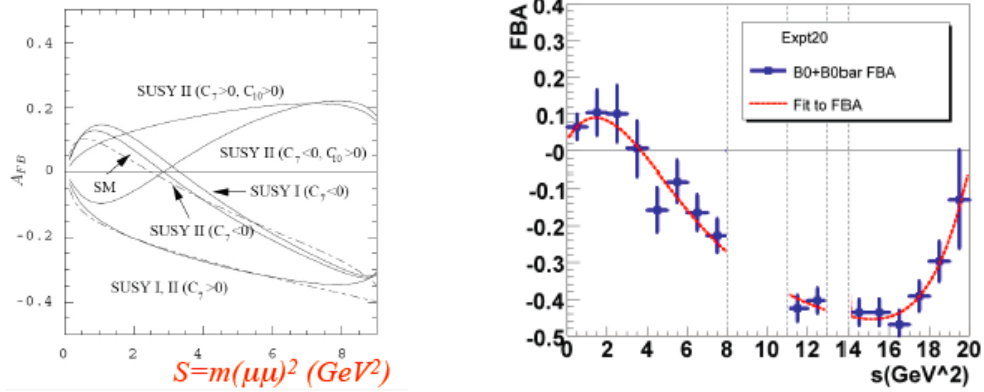


FIGURE 6. Distribution of the forward-backward asymmetry in $B_d \rightarrow K^* \mu \mu$, as a function of the $\mu \mu$ invariant mass, for different extensions of the Standard Model (left). Distribution of the forward-backward asymmetry as expected in LHCb with $10 fb^{-1}$ (right).

Tag	Tagging power
μ opposite side	0.7% - 1.8%
e opposite side	0.4% - 0.6%
K opposite side	1.6% - 2.4%
Jet/Vertex charge	0.9% - 1.3%
π same side (B^0)	0.8% - 1.0%
K same side (B_s)	2.7% - 3.3%
Combined (B^0)	4% - 5%
Combined (B_s)	7% - 9%

Mode (+ cc)	Yield	S/ B_{bb} (90%CL)
$B^0 \rightarrow D^0 (K^+ \pi^-) K^{*0}$	3.4k	> 2
$B^0 \rightarrow D^0 (K^- \pi^+) K^{*0}$	0.5k	> 0.3
$B^0 \rightarrow D^0_{CP} (K^+ K^-) K^{*0}$	0.6k	> 0.3

FIGURE 7. Tagging power (left). Annual yield and S/B ratio for the decays $B_d \rightarrow D^0 K^{*0}$ (right).

ACKNOWLEDGMENTS

The author would like to thank I. Belyaev, O. Deschamps, H. Dijkstra, R. Forty, C. R. Jones, T. Ruf, O. Schneider G. Wilkinson, and Y. Xie for their help in preparing these proceedings.

REFERENCES

1. LHCb, VELO Technical Design Report, Tech. rep., CERN/LHCC/2001-011 (2001).
2. LHCb, Inner Tracker Technical Design Report, Tech. rep., CERN/LHCC/2002-029 (2002).
3. LHCb, Outer Tracker Technical Design Report, Tech. rep., CERN/LHCC/2001-024 (2001).
4. LHCb, RICH Technical Design Report, Tech. rep., CERN/LHCC/2000-037 (2000).
5. LHCb, CALO Technical Design Report, Tech. rep., CERN/LHCC/2000-036 (2000).
6. LHCb, MUON Technical Design Report, Tech. rep., CERN/LHCC/2001-010 (2001).
7. B. Pietrzyk, "LHCb Detector Status and Commissioning," in [20].
8. C. R. Jones, "Tracking, Vertexing and Particle Identification in LHCb," in [20].
9. LHCb, Reoptimised Dector Design and Performance Technical Design Report, Tech. rep., CERN/LHCC/2003-030 (2003).
10. CDF Collaboration, *Physics Review Letters* **97**, 062003 (2006).
11. D0 Collaboration, *Physics Review Letters* **97**, 021802 (2006).
12. A. Snyder and H.R. Quinn, *Physics Review D* **48**, 2139 (1993).
13. D. Atwood, I. Dunietz, A. Soni, *Physics Review Letters* **78**, 3275 (1997).
14. D. Atwood, I. Dunietz, A. Soni, *Physics Review D* **63**, 036005 (2001).
15. M. Gronau and D. Wyler, *Physics Letters B* **265**, 172 (1991).
16. M. Battaglia, A.J. Buras, P. Gambino, A. Stocchi, *CERN-TH-2003-002* (2003).
17. R. Fleischer, *Physics Letters B* **459**, 306 (1999).
18. R. Fleischer, J. Matias, *Physics Review D* **66**, 054009 (2002).
19. T. Goto, Y. Okada, Y. Shimizu, M. Tanaka, *Physics Review D* **55**, 4273 (1997).
20. *HCP 2006 Proceedings*, 2006.